

pubs.acs.org/Biomac Article

Activities of Family 18 Chitinases on Amorphous Regenerated Chitin Thin Films and Dissolved Chitin Oligosaccharides: Comparison with Family 19 Chitinases

Guoqiang Yu, Gehui Liu, Tianyi Liu, Ethan H. Fink, and Alan R. Esker*



Cite This: Biomacromolecules 2023, 24, 566-575

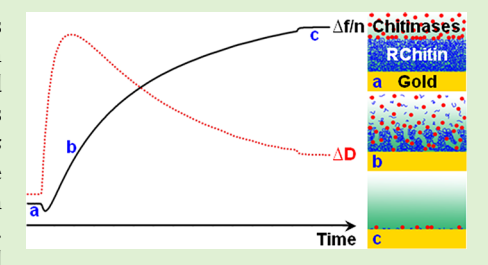


ACCESS

III Metrics & More

Article Recommendations

ABSTRACT: Changes in mass and viscoelasticity of chitin layers in fungal cell walls during chitinase attack are vital for understanding bacterial invasion of and human defense against fungi. In this work, regenerated chitin (RChitin) thin films mimicked the fungal chitin layers and facilitated studies of degradation by family 18 chitinases from *Trichoderma viride* (*T. viride*) and family 19 chitinases from *Streptomyces griseus* (*S. griseus*) that possessed chitin-binding domains (CBDs) that were absent in the family 18 chitinases. Degradation was monitored via a quartz crystal microbalance with dissipation monitoring (QCM-D) in real time at various pH and temperatures. Compared to substrates of colloidal chitin or dissolved chitin derivatives and



analogues, the degradation of RChitin films was deeply affected by chitinase adsorption. While the family 18 chitinases had greater solution activity on chitin oligosaccharides, the family 19 chitinases exhibited greater surface activity on RChitin films, illustrating the importance of CBDs for insoluble substrates.

■ INTRODUCTION

Bacteria and fungi widely exist in nature, and they are found sharing microhabitats in nearly every ecosystem. Interactions between them range from mutualism to antagonism and play important roles in ecological balance, agricultural production, and biotechnology development. 1-3 Take the fungus Rhizopus microsporus (R. microsporus) and its endosymbiont bacterium Burkholderia rhizoxinica (B. rhizoxinica) as an example. The R. microsporus harbors an endofungal bacterium, while the B. rhizoxinica assists the host in producing phytotoxin rhizoxin to kill rice plants. To enter the R. microsporus cell, the B. rhizoxinica will secrete chitinases that locally soften and loosen the fungal cell wall by degrading chitin, which is one of the major structural components. Furthermore, fungal diseases are a global health problem. More than two million people currently suffer from life-threatening fungal infections throughout the world.⁴ Worldwide, cryptococcal meningitis caused by the fungus Cryptococcus neoformans affects about 220,000 people with HIV/AIDS annually, resulting in nearly 181,000 deaths.5 Humans encode two active chitinases: chitotriosidase and acidic mammalian chitinase. 6 Chitinase levels in humans increase in response to invasive fungal infections. ^{7,8} The release of small chitin fragments generated from the digestion of chitin layers in the fungal cell walls via the chitinases leads to chitin recognition by our immune system and that further triggers immune responses. Clearly, chitinases are closely related to fungal activities, and an exploration of chitin-chitinase interactions can greatly help us understand how fungi and nature work.

Chitin is a linear homopolysaccharide composed of Nacetyl-D-glucosamine (GlcNAc) units that are connected through covalent β -(1 \rightarrow 4) linkages in which every unit is rotated 180° relative to the preceding GlcNAc unit. One end of its chain is a reducing end with a hemiacetal group that is in equilibrium with an aldehyde group, and the other is a nonreducing end with a pendant hydroxyl group. Chitin cannot be dissolved in water or common organic solvents partly due to strong inter- and intramolecular hydrogenbonding interactions among its molecules.^{9,10} In fungal cell walls, chitin molecules pack into microfibrils that are located next to the plasma membrane. The chitin layer usually has a thickness of a few nanometers and provides the fungal cell wall with indispensable structural integrity. 11-13 Chitinases are a group of hydrolytic enzymes that catalyze the degradation of chitin by breaking glycosidic bonds. Based upon the amino acid sequence and similarity, most chitinases can be categorized into family 18 and 19. Family 18 chitinases are primarily distributed in bacteria, fungi, viruses, animals, humans, and some plants, while family 19 chitinases mostly exist in plants and a few microorganisms. 14-16 The chitinases isolated from nature are usually a mixture of endochitinases

Received: April 28, 2022 Revised: September 23, 2022 Published: January 30, 2023





Figure 1. Enzymatic cleavage sites of different chitinases on chitin.

and exochitinases. 17,18 Exochitinases further contain chitobiosidases and N-acetylglucosaminidases. Endochitinases randomly cleave at internal sites in the chitin chain. Chitobiosidases and N-acetylglucosaminidases act progressively on the nonreducing end of chitin to release chitobioses and GlcNAc monomers, respectively. The combination of these chitinases leads to synergistic increases in chitinolytic activity, as shown in Figure 1.

Some researchers have studied the activity of family 18 chitinases. 19-24 Berini et al. 19 employed three dissolved fluorimetric chitin oligosaccharides, 4-methylumbelliferyl Nacetyl- β -D-glucosaminide, 4-methylumbelliferyl N,N'-diacetyl- β -D-chitobioside, and 4-methylumbelliferyl N,N',N''-triacetyl- β -D-chitotrioside, as substrates to quantify the activities of Nacetylglucosaminidase, chitobiosidase, and endochitinase in family 18 chitinases from Trichoderma viride (T. viride). Omumasaba et al.²⁰ assayed the chitinolytic activities of a purified chitinase from T. viride on partially deacetylated chitin, colloidal chitin, glycol chitin, and chitosan, respectively, using a colorimetric method. However, all of these reports focus on the enzymatic degradation of colloidal chitin or dissolved chitin derivatives and analogues in solution, and the activity of family 18 chitinases on thin chitin films has never been reported. It is presumed that the chitinases could exhibit different activities on chitin films than colloidal chitin (where the total surface area of the substrate would be greater) or dissolved chitin derivatives and analogues (with much higher substrate concentrations). In addition, the thin chitin film geometry is comparable to chitin layers in fungal cell walls, and changes in mass and viscoelasticity during degradation are anticipated to inform our understanding of how the chitinase softens the fungal cell wall to facilitate bacterium penetration.

In this work, amorphous regenerated chitin (RChitin) thin films were prepared via chemical conversion and spin-coating, and family 18 chitinases from *T. viride* were employed to degrade RChitin films for the first time at various temperatures and pH. Results were compared to family 19 chitinases from *Streptomyces griseus* (*S. griseus*). The chitinolytic activity was assayed using a quartz crystal microbalance with dissipation monitoring (QCM-D) that monitored the mass and viscoelasticity changes of the chitin films in real time. Through this study, the structural characteristics of the family 18 chitinases, the different and synergistic roles of endochitinases and exochitinases, and the effects of adsorption on hydrolysis rates were revealed.

EXPERIMENTAL SECTION

Materials. Family 18 chitinases from T. viride (lyophilized powder, ≥600 units/g solid), family 19 chitinases from S. griseus (lyophilized powder, \geq 200 units/g solid), α -chitin from shrimp shells (practical grade, $\geq 95\%$ acetylated), hydrogen peroxide (30 wt % in H₂O), 1,1,2,2-tetrachloroethane (≥98%), and chitinase assay kit, which included three chitin oligosaccharides (4-nitrophenyl N-acetyl-β-Dglucosaminide (4-NP-GlcNAc), 4-nitrophenyl N,N'-diacetyl-β-Dchitobioside $[4-NP-(GlcNAc)_2]$, and $4-nitrophenyl\ N,N',N''-triace$ tyl- β -D-chitotrioside [4-NP-(GlcNAc) $_3$]), were purchased from Sigma-Aldrich. Chloroform (HPLC grade), ammonium hydroxide (30% NH₃ in H₂O), and hydrochloric acid (HCl, 37%) were supplied by Fisher Scientific. Sodium phosphate monobasic monohydrate, sodium phosphate dibasic heptahydrate, sodium hydroxide, and phosphoric acid (≥85%) were obtained from Sigma-Aldrich and used to prepare 50 mM phosphate buffer solutions at pH 4, 6, 7, and 8, respectively. Nitrogen $(\hat{N_2}$, ultrahigh purity) was supplied by Airgas. Ultrapure water (Millipore Milli-Q, 18.2 MΩ·cm) was used for all experiments.

Preparation of Amorphous RChitin Thin Films. Due to its low solubility, chitin was first converted to trimethylsilyl chitin (TMSChitin) as previously reported. ^{25,26} Then, the TMSChitin was dissolved in a mixed solvent of chloroform and 1,1,2,2-tetrachloroethane (4:1 v/v) at a concentration of 0.7 wt %. After that, the TMSChitin solution was filtered by a syringe filter (0.45 μ m in pore size and PTFE membrane), and the filtrate was used as the spin-coating solution.

Gold-coated QCM-D sensors (QSX 301 from Biolin Scientific) were employed as the substrates for spin-coating. Prior to use, the sensors were cleaned by UV/ozone for 20 min, heated in a 5:1:1 v/v mixture of ultrapure water/hydrogen peroxide (30%)/ammonium hydroxide (30%) at 80 °C for 1 h, rinsed via ultrapure water, and dried under $\rm N_2$ gas. A thin TMSChitin film was fabricated through spin-coating 100 $\mu\rm L$ of the filtered TMSChitin solution onto a cleaned sensor surface at a spin speed of 3000 rpm for 1 min. The prepared TMSChitin film was placed face down 25 mm above the surface of a 10 wt % HCl aqueous solution for 2 min to regenerate chitin. Then, the RChitin film was rinsed with ultrapure water and dried under $\rm N_2$ gas.

Enzymatic Degradation of RChitin Films via a QCM-D. The kinetics of RChitin film degradation was monitored using a QCM-D (QSense E4, Biolin Scientific). The QCM-D sensors with RChitin films were loaded into flow modules. Then, 50 mM phosphate buffer was introduced into the system at a flow rate of 0.1 mL/min until the baseline became stable. Next, chitinases in phosphate buffer solution at a concentration of 0.2 mg/mL were injected into the system at 0.1 mL/min. After 30 min, the flow was stopped and the degradation proceeded in the absence of flow. The changes in frequency (Δf) and energy dissipation (ΔD) at the fundamental frequency and 6 odd overtones (n = 3, 5, 7, ..., 13) were recorded. When $\Delta f/n$ and ΔD versus time curves became flat, which indicated either all available RChitin was exhausted or the chitinases lost their activities, phosphate

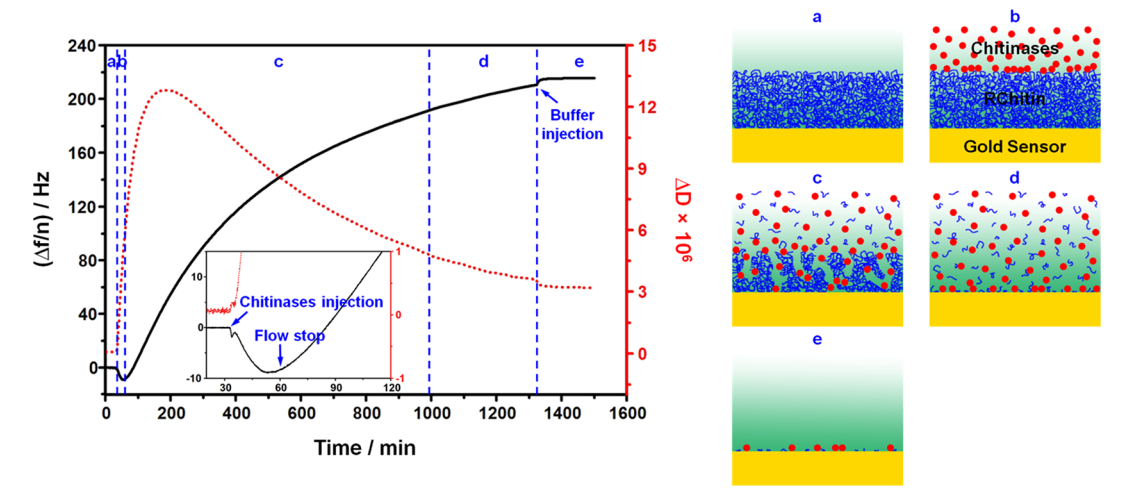


Figure 2. Representative $\Delta f/n$ (solid line) and ΔD (dotted line) versus time for the activity of family 18 chitinases on the ~20 nm thick RChitin film at 20 °C and pH 6 and a scheme for the changes in the film during this process.

buffer was flowed into the system again to wash away residual and reversibly adsorbed chitinases and degradation products. Four temperatures (20, 30, 35, and 40 $^{\circ}$ C) and four pH values (4, 6, 7, and 8) were investigated, and data from the fifth overtone (n = 5) were used for analysis.

For QCM-D measurements, if the mass on the sensor surface was evenly distributed, rigidly attached, and small relative to the mass of the quartz crystal, surface concentration Γ_{QCM} (mass per area) could be quantified using the Sauerbrey equation:

$$\Gamma_{\text{QCM}} = -C \left(\frac{\Delta f}{n} \right) \tag{1}$$

where C = 0.177 mg·m⁻²·Hz⁻¹. The decrease in frequency was proportional to the mass increase.

For viscoelastic films, the Sauerbrey equation underestimated the mass of the film. The softness of the film was related to energy dissipation (D) of the sensor, and D was defined as $^{27-29}$

$$D = \frac{E_{\text{lost}}}{2\pi E_{\text{stored}}} \tag{2}$$

where $E_{\rm lost}$ and $E_{\rm stored}$ were the energy lost and stored during a single oscillation, respectively. As a film became softer, D increased.

Enzymatic Degradation of Chitin Oligosaccharides in Solution. The activities of chitinases in solution were characterized through a colorimetric method using a chitinase assay kit, which included three chitin oligosaccharide substrates, 4-NP-GlcNAc, 4-NP-(GlcNAc)₂, and 4-NP-(GlcNAc)₃, according to the manufacturer's instructions.³⁰ The substrates were dissolved in 50 mM phosphate buffer (pH 6) at concentrations of 1 mg/mL for 4-NP-GlcNAc, 0.5 mg/mL for 4-NP-(GlcNAc)₂, and 0.2 mg/mL for 4-NP-(GlcNAc)₃. The chitinases in 50 mM phosphate buffer (pH 6) solution were prepared with a concentration of 0.01 or 1 mg/mL. Then, 100 μ L of the substrate solution and 50 μ L of the chitinase solution were sequentially added to a 96-well microplate (polystyrene, clear, and flat bottom) that was subsequently incubated in a shaker (Innova 42 from New Brunswick Scientific) at 20 °C and 160 rpm. The reaction was stopped by the addition of 200 μL of 4 wt % sodium carbonate aqueous solution. The enzymatic hydrolysis of the substrate liberated 4-nitrophenol that exhibited a yellow color under alkaline conditions that was measured with a microplate reader (Synergy Mx from BioTek Instruments) at 405 nm. A blank reaction was run, in which the chitinase solution was replaced with pure 50 mM phosphate buffer at pH 6. The activity of the chitinases was represented by the difference in absorbance between the chitinase solutions and the control.

Atomic Force Microscopy (AFM) Measurements. The QCM-D sensors were imaged in ScanAsyst mode via a Bruker Dimension

Icon atomic force microscope with a ScanAsyst-Air probe under ambient conditions (22 °C and 50% relative humidity). RChitin films were measured before, during, and after treatment by the family 18 chitinases. Films were removed from the flow modules, washed gently with water, and dried under N_2 prior to measurements. Height images with 2 × 2 μ m scan area were collected, and their root-mean-square (RMS) roughnesses were reported. The surfaces of bare gold-coated QCM-D sensors were imaged under the same conditions as a control.

Ellipsometry Measurements. Ellipsometry measurements were performed via a VASE ellipsometer (J.A. Woollam Co.) at multiple angles of incidence (60 to 80° at 2° intervals) in a spectral range of 250 to 800 nm. The resulting data were modeled using WVASE 32 software, and the thicknesses of the RChitin films were determined to be 19.8 \pm 0.8 nm.

■ RESULTS AND DISCUSSION

Activity of Family 18 Chitinases on RChitin Films. The enzymatic degradation of RChitin films by chitinases is a hydrolytic reaction, and Figure 2 shows typical QCM-D responses for this hydrolytic process. The dry RChitin film behaved as a rigid layer on the sensor surface, and it was hydrated and swelled upon contact with the phosphate buffer, as shown in Figure 2a. After the $\Delta f/n$ and ΔD baselines reached a steady state, solutions of family 18 chitinases flowed over the RChitin film. A large decrease in frequency attributed to enzyme adsorption was observed, and the small fluctuations of frequency and dissipation at the beginning of the injection of enzyme solution were believed to be caused by temporary changes in flow pressure on the sensor,³¹ as displayed in the inset of Figure 2. Once the $\Delta f/n$ vs t curve reached a minimum, $\Delta f/n$ increased, as the RChitin film was hydrolyzed into soluble GlcNAc monomers, chitobioses, and chitooligosaccharides. The slope in Figure 2 represented an apparent hydrolysis rate. The process for the film was different from colloidal chitin and dissolved chitin derivatives and analogues, where hydrolysis was fastest at the start of the experiment. For RChitin films, the maximum hydrolysis rate (the largest slope of the $\Delta f/n$ vs t curve) occurred in the middle of the degradation process. Based upon previous studies on cellulose, 32,33 the amorphous RChitin film should be porous to water but not to chitinase molecules whose molar masses range between 30 and 80 kDa.¹⁹ In other words, the chitinase molecules were confined to the surface of the RChitin film initially, as depicted in Figure 2b. As a result, the hydrolysis

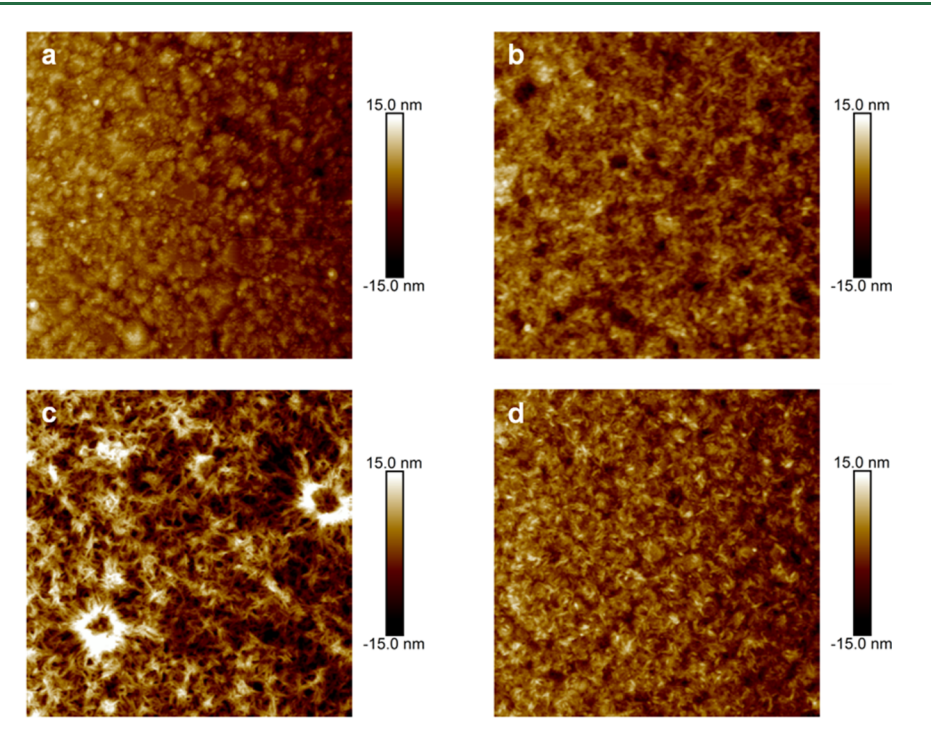


Figure 3. Representative AFM height images $(2 \times 2 \ \mu m)$ of (a) a bare gold-coated QCM-D sensor and (b-d) RChitin films before, during, and after treatment by the family 18 chitinases. The RMS roughnesses were (a) ~2.3 nm, (b) ~3.0 nm, (c) ~5.6 nm, and (d) ~3.0 nm.

rate was restricted by the limited number of nonreducing ends of RChitin chains on the film surface. Since endochitinases acted upon internal bonds of the RChitin chains, more nonreducing ends were created and exochitinase access to the film was enhanced, as shown in Figure 2c. Consequently, the hydrolysis rate increased with time, which was also an indication of the synergistic actions between the exochitinases and endochitinases. After the inflection point where the maximum hydrolysis rate was achieved, the slope of the $\Delta f/n$ vs t curve gradually decreased and plateaued. The reduced slope was due to depletion of the RChitin film, and the plateau indicated that available RChitin was totally exhausted or the chitinases lost their activities, as displayed in Figure 2d. Pure phosphate buffer was flowed over the sensor to wash away reversibly adsorbed chitinases and degradation products, which caused an additional small increase in frequency, as shown in Figure 2e.

The ΔD vs t curve reflected changes in the viscoelasticity of the RChitin film. The adsorption of chitinases and their coupled water led to an instantaneous increase in dissipation after the introduction of the chitinase solution. As the enzymatic hydrolysis took place, the endochitinase rapidly penetrated into the bulk of the film through digestion of linkages between RChitin chain ends, which caused an increase in the number of chain ends and greater hydration and swelling of the film. As a result, the film became softer with greater energy dissipation. With the synergistic actions of the endochitinases and exochitinases, the maximum dissipation was interpreted as the largest accessibility of the RChitin film to chitinase attack and has usually coincided with the maximum hydrolysis rate. 34-37 After that, the dissipation decreased due to the depletion of the RChitin film, and a plateau was reached once available RChitin was completely exhausted or the chitinases lost their activities, similar to the $\Delta f/n$ vs t curve. The final wash further reduced the dissipation, and ΔD was $\sim 3 \times 10^{-6}$ (larger than 0 in the beginning), which

was attributed to some chitinases, degradation products, or undegraded RChitin left on the sensor surface.

Representative morphological changes of RChitin films during degradation by the family 18 chitinases obtained from AFM are provided in Figure 3. A smooth and homogeneous RChitin film was fabricated with an RMS roughness of \sim 3.0 nm, as shown in Figure 3b. As some of the RChitin film was degraded, its surface became rougher and the RMS roughness increased to \sim 5.6 nm (Figure 3c), in line with Figure 2c. After hydrolysis and a buffer wash, the RMS roughness decreased to \sim 3.0 nm (Figure 3d), an indication that most of the RChitin was degraded. Since the RMS roughness in Figure 3d was greater than that in Figure 3a, some chitinases, degradation products, or undegraded RChitin must have remained on the sensor surface after the buffer wash, which was consistent with the residual ΔD in the QCM-D data in Figure 2.

Actually, the frequency and dissipation changes throughout the incubation period were the result of a variety of simultaneous factors. Substrate degradation was convoluted with enzyme adsorption, while the enzyme adsorption/ desorption was concurrent with the substrate degradation. Variations in the density and viscosity of the bulk solution surrounding the sensor could also alter the response of the QCM-D. While these factors masked the true adsorption and hydrolysis rates, the entire incubation process was clearly divided into three stages, as displayed in Figure 4. The first stage was dominated by enzyme adsorption and corresponded to a decrease in frequency and an increase in dissipation. Both the frequency and dissipation increased in the second stage and that was interpreted as enzyme penetration and hydrolysis, a result of synergistic actions of the exochitinases and endochitinases. An increase in frequency coincided with a decrease in dissipation in the final stage and that was attributed to the hydrolytic removal of the substrate. Compared to the enzyme adsorption and substrate degradation, QCM-D responses caused by changes of the liquid properties that

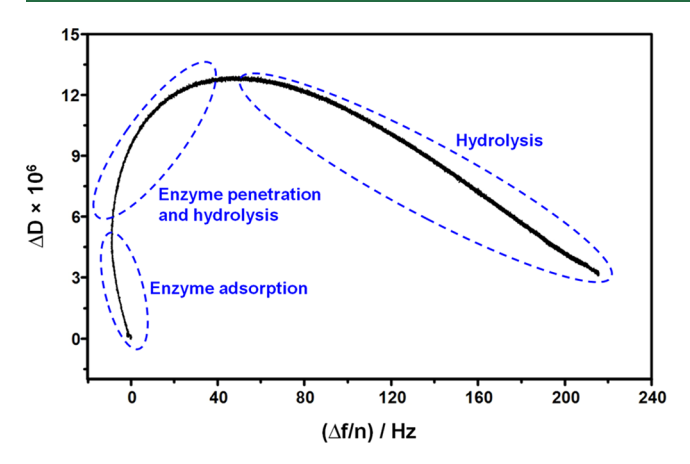
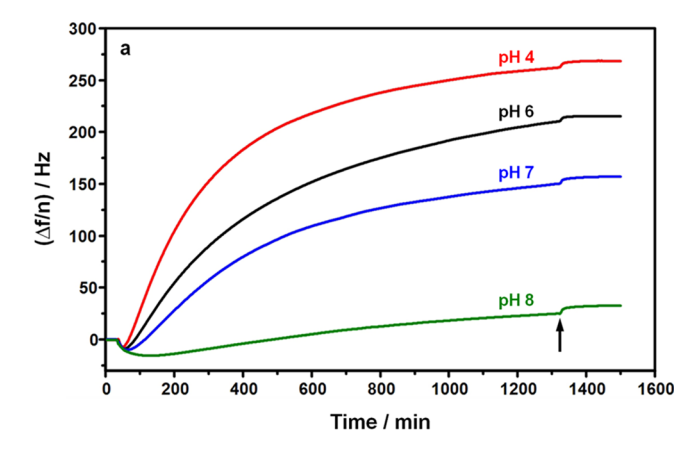


Figure 4. Representative ΔD vs $\Delta f/n$ for the activity of family 18 chitinases on the ~20 nm thick RChitin film at 20 °C and pH 6.

resulted from alternation of pure buffer and enzyme solution were negligible.^{34–36} Since the true values were convoluted, the adsorbed amount and hydrolysis rate were always regarded as apparent in our discussion.

Both the family 18 chitinases from T. viride and family 19 chitinases from S. griseus used in this work were a mixture of exochitinases (chitobiosidase and N-acetylglucosaminidase) and endochitinases that had synergistic activities. 19,38-They worked together and facilitated the degradation of the RChitin films, but their effects on QCM-D responses were different. The exochitinase acted progressively on the nonreducing ends of RChitin chains and released soluble chitobioses and GlcNAc monomers and their associated coupled water. Hence, the exochitinase caused substantial mass loss and thickness decrease that were reflected in the frequency increase. However, the exochitinase did not increase the number of chain ends, and therefore, its contribution to the change in the viscoelasticity of the RChitin film during the enzyme penetration and hydrolysis stage was limited. In the long run, the exochitinase caused a slow decrease in dissipation during the final hydrolysis stage as the RChitin film was gradually consumed. On the other hand, the endochitinase rapidly penetrated and digested within the bulk of the RChitin film through cleavage at internal sites in the RChitin chains and brought about significant increases in the number of chain ends and water content of the film. Consequently, the RChitin film became softer and the dissipation increased during the enzyme penetration and hydrolysis stage in Figure 4. Nevertheless, the endochitinase contribution to mass loss was negligible due to the compensation from the increased water content of the film and the low probability that the cleaved chitin chains were of small enough molar mass to be soluble. In summary, the exochitinases were mainly responsible for the increase in $\Delta f/n$, while the endochitinases were primarily responsible for the increase in ΔD .

Effect of pH on the Activity of Family 18 Chitinases on RChitin Films. Figure 5a depicts the effect of pH on the activity of family 18 chitinases on thin RChitin films. As the pH increased from 4 to 8, the hydrolysis rates decreased in accordance with the smaller slopes of the $\Delta f/n$ vs t curves. Moreover, the plateau $\Delta f/n$ values were also smaller at the end of the incubation period as pH increased, which indicated lesser degradation of the RChitin films. At pH 8, the RChitin film barely underwent hydrolysis over the incubation time. It could be seen from Figure 5a that the minimum in $\Delta f/n$



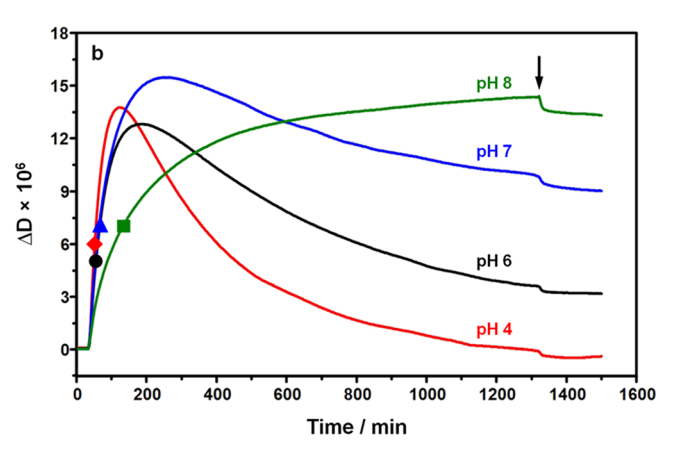


Figure 5. Representative (a) $\Delta f/n$ vs t and (b) ΔD vs t for the activity of family 18 chitinases on the ~20 nm thick RChitin film at 20 °C and various pH. The solid symbols correspond to the time when the frequency reached its minimum, for (\spadesuit) pH 4, (\spadesuit) pH 6, (\blacktriangle) pH 7, and (\blacksquare) pH 8. The arrows indicate where fresh buffer was introduced into the system at the end of the incubation.

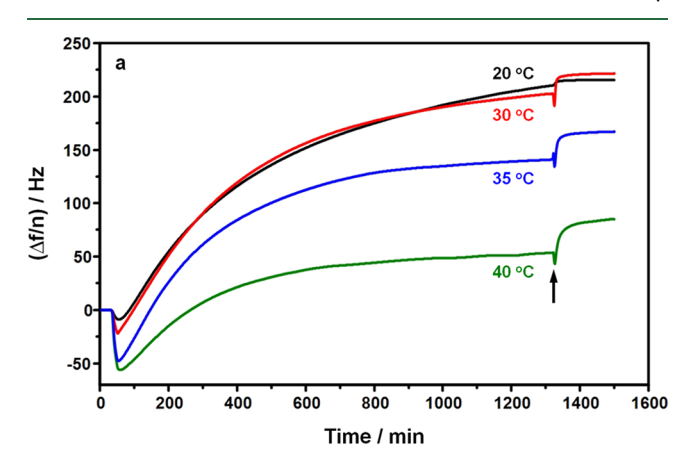
became more negative, an apparent indication of increased adsorbed chitinases with a rise in pH. This was thought to be caused by decreased activity of exochitinases that consumed lesser amounts of RChitin during the enzyme adsorption stage in Figure 4. The slopes in Figure 5a and the values of the plateaus for $\Delta f/n$ both decreased as pH increased. These observations indicated that exochitinase activity decreased with increasing pH and were consistent with greater enzyme adsorption.

In Figure 5b, ΔD was plotted as a function of time for different pH. All the maximums in ΔD at different pH were similar in magnitude \sim 13 to 15 \times 10⁻⁶ and nonzero, an indication of stable endochitinase activity across the pH range. The slopes of the ΔD vs t curves were in the order pH 4 > 6 \approx 7 \gg 8, a trend that reflected the convolution with exochitinase activity at low pH. For pH 4 through 7, there was a decrease in ΔD that corresponded to the third stage (hydrolysis) in Figure 4 where exochitinases depleted the RChitin film. The ΔD vs t curve dropped faster for the trend pH 4 > 6 > 7 and was consistent with decreased exochitinase activity as pH increased. The exochitinases lost almost all of their activity at pH 8 based upon Figure 5a, and thus, ΔD exhibited a plateau rather than a decline.

Our results that the family 18 chitinases from *T. viride* performed best in a mildly acidic environment were consistent with previous studies on colloidal chitin and dissolved chitin

derivatives and analogues. 19-22 It was found in our experiments that the family 18 chitinases quickly dissolved in pH 8 phosphate buffer, but soon became cloudy, which was probably caused by enzyme denaturation. This explained the low hydrolytic activity of family 18 chitinases under alkaline conditions. The degradation of chitin by chitinases from T. viride is believed to follow a substrate-assisted retaining mechanism. 43-45 In this mechanism, the glycosidic oxygen of chitin was first protonated by the carboxyl group of glutamic acid on the chitinase. Then, the formed oxazoline ion intermediate was stabilized by the N-acetyl group of chitin that acted as a nucleophile. Next, the glycosidic bond broke and water molecules were introduced to complete the hydrolysis reaction. Based upon this mechanism, the glutamic acid on the chitinase, which has a pK_a of 4.25, was essential for catalysis, and therefore, a mildly acidic environment promoted glycosidic oxygen protonation. Consequently, the chitinase exhibited a relatively high chitinolytic activity under mildly acidic conditions.

Effect of Temperature on the Activity of Family 18 Chitinases on RChitin Films. The QCM-D responses to temperature variations are shown in Figure 6. The $\Delta f/n$ vs t curves in Figure 6a exhibited shallower minima in $\Delta f/n$ below 100 min as the temperature decreased, an indication that lesser amounts of the chitinases were adsorbed. This observation may



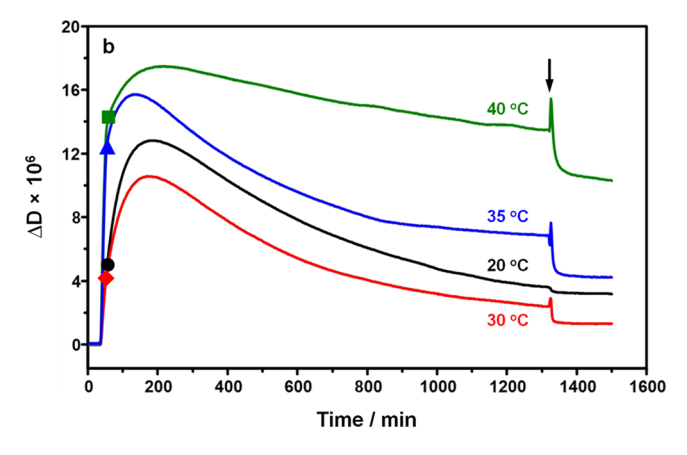


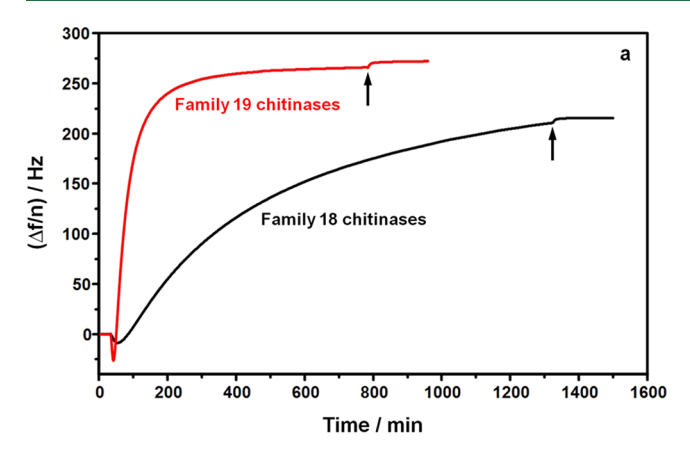
Figure 6. Representative (a) $\Delta f/n$ vs t and (b) ΔD vs t for the activity of family 18 chitinases on the ~20 nm thick RChitin film at pH 6 and various temperatures. The solid symbols correspond to the time when the frequency reached its minimum, for (\bullet) 20 °C, (\bullet) 30 °C, (\bullet) 35 °C, and (\blacksquare) 40 °C. The arrows indicate where fresh buffer was introduced into the system at the end of the incubation.

have resulted from a rougher and broader RChitin film as the RChitin film expanded and swelled with an increase in the temperature. Moreover, higher $\Delta f/n$ plateaus were observed at the end of the experiment for 20 and 30 °C than for 35 and 40 °C, which indicated greater exochitinase activity at 20 and 30 °C and greater degrees of RChitin film degradation. Although the hydrolysis rate at 35 °C was initially comparable to or even faster than that at 20 or 30 °C based upon the slopes of the $\Delta f/n$ vs t curves between \sim 60 and \sim 200 min, $\Delta f/n$ plateaued at a smaller value, which was attributed to reduced exochitinase stability at higher temperature. By 40 °C, there was an even more pronounced effect of temperature. The minimum in $\Delta f/n$ was deeper, and the plateau in $\Delta f/n$ at the end of the incubation was \sim 1/3 the value at 20 and 30 °C.

The plots of ΔD vs t in Figure 6b had three major features. The first feature was an instantaneous increase in ΔD with a slope that roughly increased with temperature. This region of the plot corresponded to the enzyme adsorption portion of the curve in Figure 4 and ended at the solid symbol that corresponded to the minimum in $\Delta f/n$ in Figure 6a. Next, Figure 6b transitioned into a broad maximum in ΔD that corresponded to the enzymatic penetration and hydrolysis region of Figure 4. Finally, there was a long decay in ΔD after the maximum in Figure 6b that corresponded to the hydrolysis phase of Figure 4. The data for 20 and 30 °C showed larger decreases in ΔD after the maximum that were consistent with higher degrees of film hydrolysis discussed for Figure 6a. At 35 and 40 °C, ΔD ended at much higher values that would be consistent with exochitinase inactivation at higher temperature and incomplete hydrolysis. Another interesting observation was that ΔD increased more significantly during the enzymatic penetration and hydrolysis stage at 20 and 30 °C than at 35 and 40 °C. A possible reason was that the endochitinase "hopped" around on the surface of the RChitin film more easily at higher temperature, which resulted in more digestion near the surface prior to penetration deep into the film. 46 The dissipation declined after its maximum as a result of the depletion of the RChitin film by the exochitinase.

As the temperature increased, greater changes in frequency and dissipation were observed when the pure phosphate buffer flowed over the sensor at the end of the incubation, as shown in Figure 6. This observation was attributed to greater desorption of chitinases and degradation products from the sensor surface on account of unfavorable adsorption at higher temperature. Compared to literature reports where the optimum temperature for the family 18 chitinases from T. viride on colloidal chitin or dissolved chitin derivatives and analogues in solution was $\sim 40~^{\circ}\text{C}$, 19,21 our findings revealed a smaller hydrolysis rate at 40 $^{\circ}\text{C}$ and a lower optimum temperature on the insoluble substrate. The discrepancy between soluble and insoluble substrates was attributed to the impacts of the stability and adsorption of the chitinases at higher temperature on the insoluble substrate.

Activity of Family 19 Chitinases on RChitin Films. A comparison of activity between family 18 chitinases and family 19 chitinases on thin RChitin films is provided in Figure 7. The family 19 chitinases showed much greater activity on the RChitin films. Starting with Figure 7a, the initial slope for $\Delta f/n$ vs t after the minimum was greater and a higher $\Delta f/n$ plateau value was achieved for family 19 chitinases. The $\Delta f/n$ plateau for the family 18 chitinases was achieved at a time \sim 5 times longer. These results indicated that the RChitin film was degraded faster and more completely by the family 19



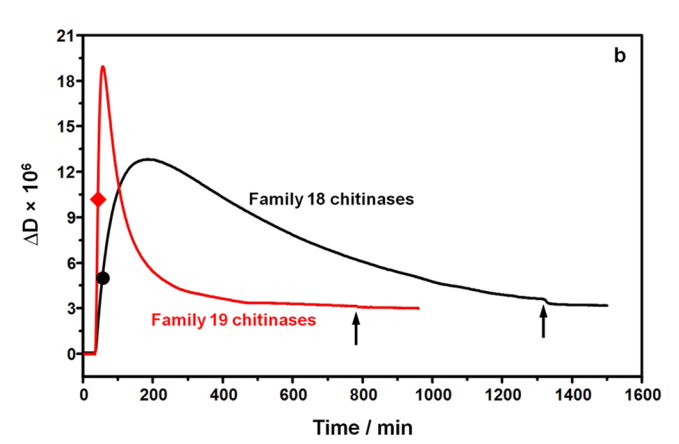


Figure 7. Representative (a) $\Delta f/n$ vs t and (b) ΔD vs t for the activity of family 18 and 19 chitinases on the ~20 nm thick RChitin film at 20 °C and pH 6. The solid symbols correspond to the time when the frequency reached its minimum, for (\bullet) family 18 chitinases and (\bullet) family 19 chitinases. The arrows indicate where fresh buffer was introduced into the system at the end of the incubation.

chitinases. Furthermore, there were substantial differences in the ΔD vs t plots for family 18 and 19 chitinases. Family 19 chitinases had a larger ΔD maximum that was achieved more quickly and decayed to the plateau value more quickly than family 18 chitinases. In addition, the minimum for $\Delta f/n$ of family 19 chitinases was deeper and was reached faster, an indication that the family 19 chitinases were adsorbed more rapidly in greater quantity during the enzyme adsorption stage in Figure 4. The reason for the difference in their QCM-D responses was thought to be that family 18 chitinases from T. viride lacked chitin-binding domains (CBDs) in their structure, whereas family 19 chitinases from S. griseus possessed CBDs. 20,47 The CBDs significantly facilitated the adsorption

of chitinases onto RChitin films, thus enhancing the hydrolysis rate. An enzymatic reaction normally begins with the enzyme binding to the substrate to form an enzyme—substrate complex, which is then broken down into the product and the original enzyme. Based upon the Michaelis—Menten kinetics model, a low concentration of enzyme—substrate complex or a low rate of enzyme—substrate complex formation can seriously retard reaction rates. Larger adsorption and faster digestion of insoluble substrates have also been reported by Cheng et al. for cellulases. Cellulases with carbohydrate-binding modules (CBMs) exhibited greater activity on insoluble cellulose than cellulases without CBMs. The studies by Cheng et al. for cellulases were consistent with greater family 19 chitinase activity than family 18 chitinase activity on RChitin films.

Activity of Chitinases on Dissolved Chitin Oligosac**charides.** To verify that the greater family 19 chitinase activity on the insoluble RChitin films did not simply arise from greater family 19 chitinase activity in solution, a chitinase assay kit, which included three soluble chitin oligosaccharides of different lengths, 4-NP-GlcNAc, 4-NP-(GlcNAc)2, and 4-NP-(GlcNAc)3, was employed to assay the chitinolytic activities of family 18 and 19 chitinases in solution. 48-50 The chitin oligosaccharides served as dimeric, trimeric, and tetrameric substrates, respectively, and contained a 4-nitrophenol group that connected to the chitooligosaccharide through a β -(1 \rightarrow 4) linkage at the reducing end of the chitin oligosaccharide. Upon cleavage, the 4-nitrophenol exhibited a yellow color. Based upon their mechanisms of action, N-acetylglucosaminidases, chitobiosidases, and endochitinases required at least a dimer, trimer, and tetramer, respectively, for the observation of hydrolytic activity. Therefore, 4-NP-GlcNAc was only degraded by N-acetylglucosaminidases, both chitobiosidases and N-acetylglucosaminidases acted on 4-NP-(GlcNAc)2, and all three classes of chitinases participated in the hydrolysis of 4-NP-(GlcNAc)₃. ^{49,51} Accordingly, the degradation of the 4-NP-(GlcNAc)₃ most closely resembled the activity of the family 18 or 19 chitinase mixtures on actual chitin.

Table 1 shows representative absorbance data for 4-nitrophenol released from 4-NP-GlcNAc, 4-NP-(GlcNAc)₂, and 4-NP-(GlcNAc)₃ upon incubation with equal amounts of family 18 and 19 chitinases. The absorbance observed for the activity of family 19 chitinases from *S. griseus* at a concentration of 0.01 mg/mL on 4-NP-GlcNAc solution was about 0 after incubation for 30 min, an indication of low *N*-acetylglucosaminidase activity, and therefore, the hydrolysis of 4-NP-(GlcNAc)₂ with an absorbance of 0.052 after 30 min was primarily achieved by the chitobiosidases in the family 19 chitinases. Since the absorbance for the 4-NP-(GlcNAc)₃ was

Table 1. Absorbance of 4-Nitrophenol Released from Hydrolysis of Chitin Oligosaccharides

substrate	chitinases	absorbance (hydrolysis time)	
4-NP-GlcNAc	family 18	$0.694 \pm 0.024 (30 \text{ min})^a$	$0.416 \pm 0.009 (18 \text{ min})^a$
	family 19	$0 \pm 0.003 (30 \text{ min})^a$	$0.385 \pm 0.005 (24 \text{ h})^b$
4-NP-(GlcNAc) ₂	family 18	$0.145 \pm 0.015 (30 \text{ min})^a$	$0.341 \pm 0.037 (90 \text{ min})^a$
	family 19	$0.052 \pm 0.006 (30 \text{ min})^a$	$0.338 \pm 0.088 (270 \text{ min})^a$
4-NP-(GlcNAc) ₃	family 18	$0.047 \pm 0.010 (30 \text{ min})^a$	$0.733 \pm 0.093 (270 \text{ min})^a$
	family 19	$0 \pm 0.003 (30 \text{ min})^a$	$0.337 \pm 0.004 (24 \text{ h})^b$

^aThe concentration of the family 18 and 19 chitinases before being added to the 96-well microplate was 0.01 mg/mL. The error bars represent one standard deviation. ^bThe concentration of the family 18 and 19 chitinases before being added to the 96-well microplate was 1 mg/mL. The error bars represent one standard deviation.

nearly 0 as well after a 30 min incubation, the endochitinases in the family 19 chitinases possessed low activity. In contrast, family 18 chitinases from T. viride exhibited stronger activity on all three substrates within 30 min. For 4-NP-GlcNAc and 4-NP-(GlcNAc)₃, the concentration of the family 19 chitinase solution was increased by a factor of 100, without detectable activity in 30 min. Only after a 24 h incubation time with 1 mg/mL solutions of family 19 chitinases was appreciable activity observed on 4-NP-GlcNAc and 4-NP-(GlcNAc), (roughly half of what was observed for ~30 and ~270 min reaction times with family 18 chitinases at 0.01 mg/mL, respectively). These results indicated that the family 19 chitinases had very low N-acetylglucosaminidase and endochitinase activity in solution relative to the family 18 chitinases. With the exception of family 18 chitinases in 4-NP-(GlcNAc)₃ solution, all other solutions showed absorbances that increased at a steady or slowing rate over the time range investigated. In contrast, the 4-NP-(GlcNAc)₃ solution with family 18 chitinases exhibited a lag phase followed by an acceleration in the growth rate of absorbance, which may have been caused by substrate inhibition in the initial stage of degradation. 52

While it was difficult to distinguish the relative activities of endochitinases and exochitinases in family 18 chitinases from T. viride and family 19 chitinases from S. griseus because most of the substrates were acted upon by more than one type of enzyme, absorbance and time data clearly showed that the family 18 chitinases had greater activity on all three substrates after the same 30 min of incubation and the family 19 chitinases exhibited much less activity even for longer incubation times at higher concentration (the family 19 chitinases at a 100 times higher concentration required more than 5 times as long as the family 18 chitinases for appreciable degradation of the 4-NP-(GlcNAc)₃ in solution). In contrast, QCM-D experiments for family 18 and 19 chitinases at equal concentration clearly showed that the family 19 chitinases had far greater activity on insoluble substrates (the family 18 chitinases required ~5 times longer than the family 19 chitinases for degradation of the RChitin film). The studies on soluble substrates clearly showed that the family 18 chitinases did not possess inherently weaker activity at equivalent concentration in solution and that greater family 19 chitinase activity on RChitin films must arise from a different source. Thus, the existence of CBDs in family 19 chitinases was strongly suspected as the cause of the enhanced activity.

This study was not the first to explore the role of CBDs. Work by Suginta et al. produced a recombinant CBD from Vibrio harveyi chitinase A, a GH-18 glycosyl hydrolase, and demonstrated that the binding domain bound colloidal α - and β -chitin.⁵³ However, the binding domain alone had significantly lower binding affinity than the wild-type chitinase, an indication of a role for the catalytic domain in the binding process. Studies by Takashima et al. used complementary DNA cloning and expression to produce chitinase from Ficus microcarpa and a variant that lacked the CBD.⁵⁴ The variant showed lower quantitative activity on glycol chitin in solution and qualitatively lower activity on the surface of the fungus T. viride via microscopy than the wild-type chitinase. This study showed the importance of the binding domain for catalytic activity, with both decreased solution and surface activity upon the removal of the CBD. Similarly, work by Xu and Zhang used recombinant chitotriosidases from *Branchiostoma japonicum* with and without binding domains. ⁵⁵ They observed that the removal of the CBD greatly diminished solution activity on 4-

methylumbelliferyl- β -D-N,N',N''-triacetylchitotrioside, both versions of the chitotriosidase bound chitin powder as observed qualitatively through SDS-PAGE analyses, and the full enzyme exhibited growth inhibition for the fungus Candida albicans that was absent without the CBD. In work by Minamihata et al., recombinant biology techniques were used to make chitinase A from *Pteris ryukyuensis*. ⁵⁶ A polymerizable version of the recombinant enzyme as well as polymers with various combinations of the chitin-binding and catalytic domains was made. The monomeric and polymeric analogue of the wild-type enzyme showed greater solution activity on glycol chitin, with similar initial activity on chitin powder. Removal of the CBDs to form monomers and polymers with only catalytic domains lowered chitinase activity on glycol chitin and chitin powder and decreased antifungal activity against T. viride. In this study, the difference in solution and surface activity between the family 18 chitinases from T. viride and family 19 chitinases from S. griseus was attributed to a lack of CBDs for the T. viride sample. However, based upon the studies reviewed in this paragraph, decreased solution activity should have matched decreased surface activity that was clearly not observed. In fact, there was a complete reversal in activity for the two systems between the solution and the surface. Moreover, there was a retention of some surface activity for the enzymes from T. viride believed to lack CBDs. The use of QCM-D with a fully degradable chitin, RChitin, allowed rapid quantification of enzymatic degradation on a well-defined insoluble surface. Application of this technique to recombinant chitinases would be a next logical step for understanding differences in chitinase activity on surfaces and in solution.

CONCLUSIONS

This work highlighted the chitinolytic activity of family 18 chitinases from T. viride on thin RChitin films at various pH and temperatures using QCM-D that monitored the changes in mass and viscoelasticity of the films in real time throughout the degradation process. Based upon the frequency and dissipation changes, the degradation process in a typical experiment could be divided into three stages, enzyme adsorption, enzyme penetration and hydrolysis, and hydrolysis. The variations in the activity of the family 18 chitinases along with the changes in pH were consistent with literature reports that they preferred an acidic environment, but our work also found that the endochitinase was clearly more stable than the exochitinase in terms of activity at different pH. The optimum temperature for the activity of the family 18 chitinases was around 30 °C, which was lower than that reported in the literature for the degradation of colloidal chitin or dissolved chitin derivatives and analogues, which may have resulted from the differences in stability and adsorption of chitinases at high temperature on different substrates. This work also compared the activities of the family 18 and 19 chitinases from T. viride and S. griseus, respectively, on RChitin films and dissolved chitin oligosaccharides for the first time. They exhibited completely opposite and vastly different degradation performances. The family 18 chitinases from T. viride possessed a much lower activity on thin RChitin films but a significantly greater activity on dissolved chitin oligosaccharides in solution. This difference in solution versus surface activity was attributed to the lack of CBDs in their structures and indicated the importance of CBDs for chitinase activity on insoluble substrates. These results are expected to provide insights into chitinase activity on fungal cell walls.

AUTHOR INFORMATION

Corresponding Author

Alan R. Esker — Department of Chemistry and Macromolecules Innovation Institute, Virginia Tech, Blacksburg, Virginia 24061, United States; oocid.org/0000-0003-1440-5933; Phone: (540) 239-1611; Email: aesker@vt.edu

Authors

Guoqiang Yu — Department of Chemistry, Virginia Tech, Blacksburg, Virginia 24061, United States; orcid.org/ 0000-0003-1781-8856

Gehui Liu – Department of Chemistry, Virginia Tech, Blacksburg, Virginia 24061, United States

Tianyi Liu — Department of Chemistry, Virginia Tech, Blacksburg, Virginia 24061, United States

Ethan H. Fink – Department of Chemistry, Virginia Tech, Blacksburg, Virginia 24061, United States

Complete contact information is available at: https://pubs.acs.org/10.1021/acs.biomac.2c00538

Notes

The authors declare no competing financial interest.

■ ACKNOWLEDGMENTS

This work was supported by GlycoMIP, a National Science Foundation Materials Innovation Platform funded through Cooperative Agreement DMR-1933525.

REFERENCES

- (1) Deveau, A.; Bonito, G.; Uehling, J.; Paoletti, M.; Becker, M.; Bindschedler, S.; Hacquard, S.; Hervé, V.; Labbé, J.; Lastovetsky, O. A.; Mieszkin, S.; Millet, L. J.; Vajna, B.; Junier, P.; Bonfante, P.; Krom, B. P.; Olsson, S.; van Elsas, J. D.; Wick, L. Y. Bacterial-fungal interactions: ecology, mechanisms and challenges. *FEMS Microbiol. Rev.* 2018, 42, 335–352.
- (2) Moebius, N.; Uzum, Z.; Dijksterhuis, J.; Lackner, G.; Hertweck, C. Active invasion of bacteria into living fungal cells. *Elife* **2014**, 3, No. e03007.
- (3) Krüger, W.; Vielreicher, S.; Kapitan, M.; Jacobsen, I. D.; Niemiec, M. J. Fungal-bacterial interactions in health and disease. *Pathogens* **2019**, *8*, 70.
- (4) Kang, X.; Kirui, A.; Muszyński, A.; Widanage, M. C. D.; Chen, A.; Azadi, P.; Wang, P.; Mentink-Vigier, F.; Wang, T. Molecular architecture of fungal cell walls revealed by solid-state NMR. *Nat. Commun.* 2018, 9, 2747.
- (5) Rajasingham, R.; Smith, R. M.; Park, B. J.; Jarvis, J. N.; Govender, N. P.; Chiller, T. M.; Denning, D. W.; Loyse, A.; Boulware, D. R. Global burden of disease of HIV-associated cryptococcal meningitis: an updated analysis. *Lancet Infect. Dis.* **2017**, *17*, 873–881.
- (6) Ohno, M.; Togashi, Y.; Tsuda, K.; Okawa, K.; Kamaya, M.; Sakaguchi, M.; Sugahara, Y.; Oyama, F. Quantification of chitinase mRNA levels in human and mouse tissues by real-time PCR: species-specific expression of acidic mammalian chitinase in stomach tissues. *PLoS One* **2013**, *8*, No. e67399.
- (7) Wiesner, D. L.; Specht, C. A.; Lee, C. K.; Smith, K. D.; Mukaremera, L.; Lee, S. T.; Lee, C. G.; Elias, J. A.; Nielsen, J. N.; Boulware, D. R.; Bohjanen, P. R.; Jenkins, M. K.; Levitz, S. M.; Nielsen, K. Chitin recognition via chitotriosidase promotes pathologic type-2 helper T cell responses to cryptococcal infection. *PLoS Pathog.* **2015**, *11*, No. e1004701.
- (8) Vega, K.; Kalkum, M. Chitin, chitinase responses, and invasive fungal infections. *Int. J. Microbiol.* **2012**, 2012, No. 920459.
- (9) Wang, C.Renewable natural polymer thin films and their interactions with biomacromolecules; Ph.D. Dissertation, Virginia Tech: Blacksburg, VA 2014.

- (10) Rinaudo, M. Chitin and chitosan: properties and applications. *Prog. Polym. Sci.* **2006**, *31*, 603–632.
- (11) Bowman, S. M.; Free, S. J. The structure and synthesis of the fungal cell wall. *BioEssays* **2006**, 28, 799–808.
- (12) Gow, N. A. R.; Latge, J. P.; Munro, C. A. The fungal cell wall: structure, biosynthesis, and function. *Microbiol. Spectr.* **2017**, *5*, 5.
- (13) Free, S. J. Fungal cell wall organization and biosynthesis. *Adv. Genet.* **2013**, *81*, 33–82.
- (14) Eijsink, V.; Hoell, I.; Vaaje-Kolstada, G. Structure and function of enzymes acting on chitin and chitosan. *Biotechnol. Genet. Eng. Rev.* **2010**, *27*, 331–366.
- (15) Kawase, T.; Yokokawa, S.; Saito, A.; Fujii, T.; Nikaidou, N.; Miyashita, K.; Watanabe, T. Comparison of enzymatic and antifungal properties between family 18 and 19 chitinases from *S.coelicolor A3*(2). *Biosci., Biotechnol., Biochem.* **2006**, 70, 988–998.
- (16) Garcia-Casado, G.; Collada, C.; Allona, I.; Casado, R.; Pacios, L. F.; Aragoncillo, C.; Gomez, L. Site-directed mutagenesis of active site residues in a class I endochitinase from chestnut seeds. *Glycobiology* **1998**, *8*, 1021–1028.
- (17) Rathore, A. S.; Gupta, R. D. Chitinases from bacteria to human: properties, applications, and future perspectives. *Enzyme Res.* **2015**, 2015, 791907.
- (18) Liu, J.Studies of macromolecule/molecule adsorption and activity at solid surfaces. Ph.D. Dissertation, Virginia Tech: Blacksburg, VA, 2019.
- (19) Berini, F.; Caccia, S.; Franzetti, E.; Congiu, T.; Marinelli, F.; Casartelli, M.; Tettamanti, G. Effects of *Trichoderma viride* chitinases on the peritrophic matrix of Lepidoptera. *Pest Manage. Sci.* **2016**, *72*, 980–989.
- (20) Omumasaba, C. A.; Yoshida, N.; Ogawa, K. Purification and characterization of a chitinase from *Trichoderma viride*. J. Gen. Appl. Microbiol. 2001, 47, 53–61.
- (21) Jenifer, S.; Jeyasree, J.; Laveena, D. K.; Manikandan, K. Purification and characterization of chitinase from *Trichoderma viride* N9 and its antifungal activity against phytopathogenic fungi. *World. J. Pharm. Pharm. Sci.* **2014**, *3*, 1604–1611.
- (22) da Silva, L. C. A.; Honorato, T. L.; Cavalcante, R. S.; Franco, T. T.; Rodrigues, S. Effect of pH and temperature on enzyme activity of chitosanase produced under solid stated fermentation by *Trichoderma* spp. *Indian. J. Microbiol.* **2012**, *52*, 60–65.
- (23) Mallikharjuna Rao, K. L. N.; Siva Raju, K.; Ravisankar, H. Cultural conditions on the production of extracellular enzymes by *Trichoderma* isolates from tobacco rhizosphere. *Braz. J. Microbiol.* **2016**, 47, 25–32.
- (24) Ekundayo, E. A.; Ekundayo, F. O.; Bamidele, F. Production, partial purification and optimization of a chitinase produced from *Trichoderma viride*, an isolate of maize cob. *Mycosphere* **2016**, *7*, 786–793.
- (25) Kurita, K.; Sugita, K.; Kodaira, N.; Hirakawa, M.; Yang, J. Preparation and evaluation of trimethylsilylated chitin as a versatile precursor for facile chemical modifications. *Biomacromolecules* **2005**, *6*, 1414–1418.
- (26) Kittle, J. D.; Wang, C.; Qian, C.; Zhang, Y.; Zhang, M.; Roman, M.; Morris, J. R.; Moore, R. B.; Esker, A. R. Ultrathin chitin films for nanocomposites and biosensors. *Biomacromolecules* **2012**, *13*, 714–718
- (27) Dixon, M. C. Quartz crystal microbalance with dissipation monitoring: enabling real-time characterization of biological materials and their interactions. *J. Biomol. Tech* **2008**, *19*, 151–158.
- (28) Zhang, X.Adsorption of biomacromolecules onto polysaccharide surfaces; Ph.D. Dissertation, Virginia Tech: Blacksburg, VA, 2014. (29) Chen, Q.; Xu, S.; Liu, Q.; Masliyah, J.; Xu, Z. QCM-D study of nanoparticle interactions. *Adv. Colloid Interface Sci.* **2016**, 233, 94–
- (30) Chitinase Assay Kit. https://www.sigmaaldrich.com/US/en/product/sigma/cs0980 (accessed July 2, 2022).
- (31) Rojas, O. J.; Jeong, C.; Turon, X.; Argyropoulos, D. S.Measurement of cellulase activity with piezoelectric resonators. In Materials, chemicals, and energy from forest biomass; Argyropoulos, D.

- S., Ed.; American Chemical Society: Washington, DC, 2007; Vol. 954, pp. 478–494.
- (32) Kittle, J. D.; Qian, C.; Edgar, E.; Roman, M.; Esker, A. R. Adsorption of xyloglucan onto thin films of cellulose nanocrystals and amorphous cellulose: film thickness effects. ACS Omega 2018, 3, 14004–14012.
- (33) Kittle, J. D.; Du, X.; Jiang, F.; Qian, C.; Heinze, T.; Roman, M.; Esker, A. R. Equilibrium water contents of cellulose films determined via solvent exchange and quartz crystal microbalance with dissipation monitoring. *Biomacromolecules* **2011**, *12*, 2881–2887.
- (34) Wang, C.; Kittle, J. D.; Qian, C.; Roman, M.; Esker, A. R. Chitinase activity on amorphous chitin thin films: a quartz crystal microbalance with dissipation monitoring and atomic force microscopy study. *Biomacromolecules* **2013**, *14*, 2622–2628.
- (35) Hu, G.; Heitmann, J. A., Jr.; Rojas, O. J. In situ monitoring of cellulase activity by microgravimetry with a quartz crystal microbalance. *J. Phys. Chem. B* **2009**, *113*, 14761–14768.
- (36) Turon, X.; Rojas, O. J.; Deinhammer, R. S. Enzymatic kinetics of cellulose hydrolysis: a QCM-D study. *Langmuir* **2008**, *24*, 3880–3887
- (37) Liu, J.; Zhu, Y.; Wang, C.; Goodell, B.; Esker, A. R. Chelator-mediated biomimetic degradation of cellulose and chitin. *Int. J. Biol. Macromol.* **2020**, *153*, 433–440.
- (38) Chitinase from Trichoderma viride. https://www.sigmaaldrich.com/US/en/product/sigma/c8241 (accessed July 2, 2022).
- (39) Chitinase from Streptomyces griseus. https://www.sigmaaldrich.com/US/en/product/sigma/c6137 (accessed July 2, 2022).
- (40) Kim, K.; Ji, H.-S. Effect of chitin sources on production of chitinase and chitosanase by *Streptomyces griseus* HUT 6037. *Biotechnol. Bioprocess Eng.* **2001**, *6*, 18–24.
- (41) Tanabe, T.; Morinaga, K.; Fukamizo, T.; Mitsutomi, M. Novel chitosanase from *Streptomyces griseus* HUT 6037 with transglycosylation activity. *Biosci., Biotechnol., Biochem.* **2003**, 67, 354–364.
- (42) Mitsutomi, M.; Hata, T.; Kuwahara, T. Purification and characterization of novel chitinases from *Streptomyces griseus* HUT 6037. *J. Ferment. Bioeng.* **1995**, *80*, 153–158.
- (43) Brameld, K. A.; Shrader, W. D.; Imperiali, B.; Goddard, W. A., III Substrate assistance in the mechanism of family 18 chitinases: theoretical studies of potential intermediates and inhibitors. *J. Mol. Biol.* **1998**, *280*, 913–923.
- (44) Tews, I.; Terwisscha van Scheltinga, A. C.; Perrakis, A.; Wilson, K. S.; Dijkstra, B. W. Substrate-assisted catalysis unifies two families of chitinolytic enzymes. *J. Am. Chem. Soc.* **1997**, *119*, 7954–7959.
- (45) Oyeleye, A.; Normi, Y. M. Chitinase: diversity, limitations, and trends in engineering for suitable applications. *Biosci. Rep.* **2018**, 38, BSR2018032300.
- (46) Cheng, G.; Datta, S.; Liu, Z.; Wang, C.; Murton, J. K.; Brown, P. A.; Jablin, M. S.; Dubey, M.; Majewski, J.; Halbert, C. E.; Browning, J. F.; Esker, A. R.; Watson, B. J.; Zhang, H.; Hutcheson, S. W.; Huber, D. L.; Sale, K. L.; Simmons, B. A.; Kent, M. S. Interactions of endoglucanases with amorphous cellulose films resolved by neutron reflectometry and quartz crystal microbalance with dissipation monitoring. *Langmuir* 2012, 28, 8348–8358.
- (47) Itoh, Y.; Watanabe, J.; Fukada, H.; Mizuno, R.; Kezuka, Y.; Nonaka, T.; Watanabe, T. Importance of Trp59 and Trp60 in chitin-binding, hydrolytic, and antifungal activities of *Streptomyces griseus* chitinase C. *Appl. Microbiol. Biotechnol.* **2006**, 72, 1176–1184.
- (48) Guigón López, C.; Muñoz Castellanos, L. N.; Flores Ortiz, N. A.; González González, J. A. Control of powdery mildew (*Leveillula taurica*) using *Trichoderma asperellum* and *Metarhizium anisopliae* in different pepper types. *BioControl* **2019**, 64, 77–89.
- (49) Tronsmo, A.; Harman, G. E. Detection and quantification of N-acetyl- β -D-glucosaminidase, chitobiosidase, and endochitinase in solutions and on gels. *Anal. Biochem.* **1993**, 208, 74–79.
- (50) Herma Renkema, G.; Boot, R. G.; Muijsers, A. O.; Donker-Koopman, W. E.; Aerts, J. M. F. G. Purification and characterization of human chitotriosidase, a novel member of the chitinase family of proteins. *J. Biol. Chem.* **1995**, *270*, 2198–2202.

- (51) Haran, S.; Schickler, H.; Oppenheim, A.; Chet, I. New components of the chitinolytic system of *Trichoderma harzianum*. *Mycol. Res.* **1995**, *99*, 441–446.
- (52) Manual of clinical enzyme measurements; Worthington Biochemical Corporation: Freehold, NJ, 1972.
- (53) Suginta, W.; Sirimontree, P.; Sritho, N.; Ohnuma, T.; Fukamizo, T. The chitin-binding domain of a GH-18 chitinase from *Vibrio harveyi* is crucial for chitin-chitinase interactions. *Int. J. Biol. Macromol.* **2016**, *93*, 1111–1117.
- (54) Takashima, T.; Henna, H.; Kozome, D.; Kitajima, S.; Uechi, K.; Taira, T. cDNA cloning, expression, and antifungal activity of chitinase from *Ficus microcarpa* latex: difference in antifungal action of chitinase with and without chitin-binding domain. *Planta* **2021**, 253, 120.
- (55) Xu, N.; Zhang, S. Identification, expression and bioactivity of a chitotriosidase-like homolog in amphioxus: dependence of enzymatic and antifungal activities on the chitin-binding domain. *Mol. Immunol.* **2012**. *51*. 57–65.
- (56) Minamihata, K.; Tanaka, Y.; Santoso, P.; Goto, M.; Kosome, D.; Taira, T.; Kamiya, N. Orthogonal enzymatic conjugation reactions create chitin binding domain grafted chitinase polymers with enhanced antifungal activity. *Bioconjugate Chem.* **2021**, *32*, 1688–1698.

□ Recommended by ACS

Effects of the Structure and Molecular Weight of Alkali–Oxygen Lignin Isolated from Rice Straw on the Growth of Maize Seedlings

Dandan Wu, Yongcan Jin, et al.

FEBRUARY 17, 2023

BIOMACROMOLECULES

READ 🖸

Human Glucosylceramide Synthase at Work as Provided by "In Silico" Molecular Docking, Molecular Dynamics, and Metadynamics

Giorgia Canini, Alessandro Arcovito, et al.

FEBRUARY 22, 2023

ACS OMEGA

READ 🗹

Kinetic Characterization of a Lytic Polysaccharide Monooxygenase Reveals a Unique Specificity for Depolymerization at β-O-4 of Lignin Compounds

Simran Bhatia, Sudesh Kumar Yadav, et al.

MARCH 10, 2023

ACS SUSTAINABLE CHEMISTRY & ENGINEERING

READ 🗹

Biomimetic SARS-CoV-2 Spike Protein Nanoparticles

Alvin Phan, J. Andrew MacKay, et al.

MARCH 31, 2023

BIOMACROMOLECULES

READ 🗹

Get More Suggestions >